Alberta Energy Regulator

Outcrop of the Middle Devonian Keg River Formation on the Firebag River, Northeastern Alberta (NTS 74E/11)

AGS
ALBERTA GEOLOGICAL SURVEY

Outcrop of the Middle Devonian Keg River Formation on the Firebag River, Northeastern Alberta (NTS 74E/11)

C.L. Schneider[1], M. Grobe[2] and L.R. Leighton[3]

[1] Formerly of the Alberta Energy Regulator / Alberta Geological Survey (see page iii for current address)
[2] Alberta Energy Regulator
  Alberta Geological Survey
[3] Department of Earth and Atmospheric Sciences, University of Alberta

February 2018

Author addresses:

C.L. Schneider
Department of Earth & Atmospheric Sciences
University of Alberta
Edmonton, AB T6G 2E3
Canada
780.628.4384
E-mail: clschnei@ualberta.ca

L.R. Leighton
Department of Earth & Atmospheric Sciences
University of Alberta
Edmonton, AB T6G 2E3
Canada
780.492.3983
E-mail: lleighto@ualberta.ca

Contents

Figures

Acknowledgements

Abstract

This report contains the description of an outcrop of the Middle Devonian Keg River Formation along the north bank of the Firebag River west of the Fort Chipewyan winter road bridge. Field descriptions are supplemented with the results of thin-section analyses on six samples from the outcrop, providing additional information on composition, textures, and porosity of the rocks. The outcrop consists of a basal unfossiliferous dolostone containing no other defining features, a series of laminated and tabular-bedded dolostone beds originating from a lagoonal to intertidal paleoenvironment, and a capping stromatoporoid-rich biostromal to biohermal dolostone.

Post-depositional alteration processes interpreted from outcrop and thin-section observations include marine cementation, recrystallization, dolomitization, dissolution, fracturing, hydrocarbon migration, and late-stage calcite cementation. Dolomitization of the original limestone obscured, but did not completely obliterate, original sedimentary structures. Observed porosity types include inter- and intraparticle, intercrystalline, and solution-enlarged porosity. Porosity values range between 10% and 46%, with the values of >20% found in dolomitized peloidal and fragmental grainstone, and stromatoporoid bindstone in the biostromal to biohermal part of the outcrop.

1 Introduction and Geological Background

In August 2011, Alberta Geological Survey (AGS) stratigraphers and a palaeontologist from the University of Alberta visited the Firebag River in the Athabasca Oil Sands Area in northeastern Alberta to examine outcrops of Elk Point and Beaverhill Lake group strata. The description of the Beaverhill Lake Group outcrop (assigned to the Firebag Member of the Waterways Formation) was included in an earlier report (Schneider et al., 2014a). Herein, we present the description of an outcrop of Keg River Formation from the north bank of the Firebag River east of the Fort Chipewyan winter road bridge (Figures 1 and 2).
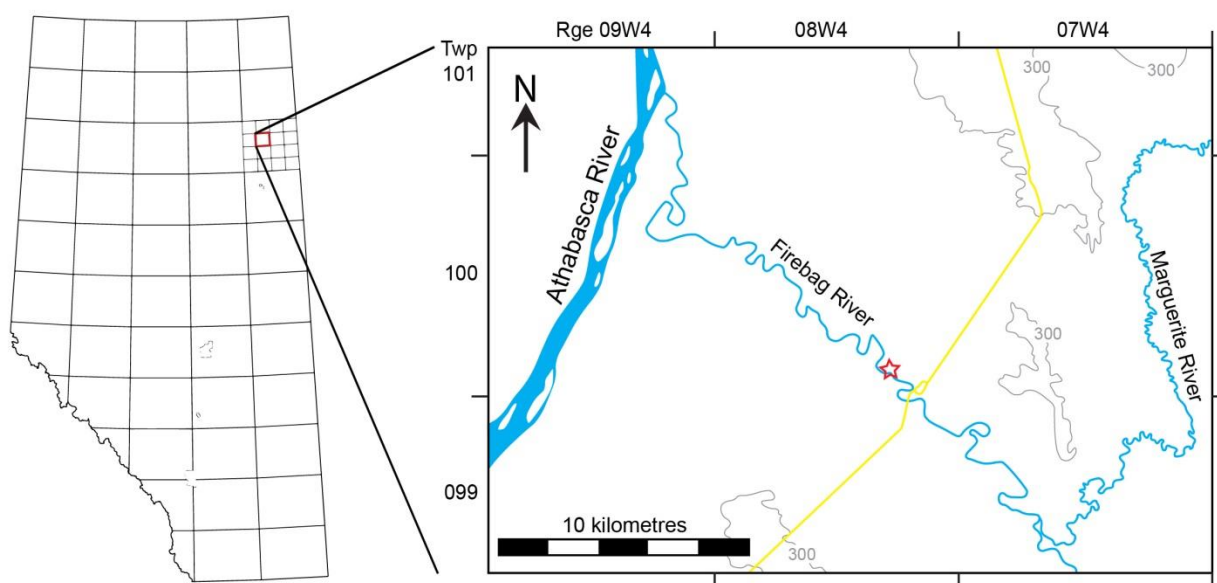
Figure 1. Location of the Keg River Formation outcrop (red star) on the Firebag River in northeastern Alberta. Red box on the inset map on the left is the footprint of NTS map sheet 74E/11 shown on the detail map on the right. The yellow line on the detail map is the winter road between Fort McMurray and Fort Chipewyan. Grey contour lines outline topographic highs.

Norris (1963) and Green et al. (1970) identified an area of Methy Formation outcrops on the Firebag River near its confluence with the Athabasca River without providing any specific descriptions. Altosaar (pers. comm., 2012) described a Keg River Formation outcrop on the Firebag River as a shallowing-upward sequence consisting of: 1) a finely crystalline, wave-rippled to planar laminated peloidal dolostone; 2) a very finely crystalline, algal dolostone with possible stromatoporoids, and 3) intact and solution-brecciated stromatolitic dolostone. Altosaar interpreted the paleoenvironment of the Keg River Formation for the outcrops along the Firebag River as a low-energy, shallow water environment that was subject to periodic subaerial exposure and stressful environmental conditions.

Keg River Formation outcrops are better known from the Clearwater River, through journal notes of early explorers and descriptions of outcrops by stratigraphers such as Norris (1963). Along the Clearwater River near the Saskatchewan and Alberta border, the Keg River Formation is a dolostone containing three main facies (Schneider et al., 2013):

- an intertidal facies of laminated dolostone that can contains stromatolites, oncoids, subaerial exposure surfaces, caliche horizons, and breccias;

- a non-biohermal, subtidal, open-platform facies of brachiopod and crinoid floatstone to rudstone; and

- a biostromal to biohermal facies of rudstone containing stromatoporoids and occasionally corals, in which fossils are typically dissolved to form large vugs.

Within the Athabasca Oil Sands region, investigations of drill core indicate that the thicker sections of the Keg River Formation contain all three facies, whereas thinner intervals contain only intertidal and subtidal, non-biohermal carbonate (Schneider and Grobe, 2013; Schneider et al., 2014b). At the outcrop on the Firebag River described herein, the Keg River Formation contains the biohermal and intertidal facies. The laminated to stromatolitic intertidal facies is exposed between the capping biohermal facies and a nondescript dolostone at the base of the outcrop.

Unlike in other Keg River Formation outcrops along the Clearwater River, the fossils and sedimentary structures in the outcrop described here were not obliterated by the dolomitization process, although the details of internal skeletal structures are lost. Massive, bulbous and tabular stromatoporoids are preserved intact and in life positions, with laminar stromatoporoids binding interstitial skeletal sand.

2 Keg River Formation, Firebag River

2.1 Locality Description and Access

UTM Zone 12, 487916E, 6389840N (NAD83)

The outcrop forms an approximately 100 m long, grey dolostone bench along the north bank of the Firebag River, about 1.5 km northwest of the Fort Chipewyan winter road bridge (Figures 1 and 2).

Figure 2. Aerial view of the Keg River Formation outcrop on the Firebag River. View is in the downstream direction. Numbers 2 to 6 label units described in Section 2.2 and illustrated in Figure 5. Unit 1 outcrops at water level to the right of the field of view. Units 4 and 5 form bench tops causing the units to appear thicker in the photograph.

The outcrop can either be accessed by helicopter landing on the dolostone bench or by quad along the winter road to the north bank of the Firebag River followed by a short hike downstream.

Several small, sulphurous springs discharge from the outcrop. The largest is at the downstream end of the outcrop, which during the 2011 visit, was exposed above river level (Figure 3). This spring had several points of discharge along a bedding plane.

The outcrop is pervasively fractured. Fracture surfaces are inclined (45 degrees) to vertical and mostly dip to the east. Glacial striae are preserved on the intermittently-exposed surface of the outcrop in the forest edge (Figure 4).

Figure 3. Sulphur springs at the downstream end of the Keg River Formation outcrop on the Firebag River. View is in the downstream direction.

Figure 4. Glacial striae on the surface of the Keg River Formation outcrop on the Firebag River. This small exposure is about 5 m from the river bank within the edge of the forest. Red arrows show the orientation of striae.

2.2 Stratigraphy

Measurements were taken at the upstream end of the outcrop (Figure 2). From base to top at this location, the outcrop contains the following units (Figure 5):

- unit 1 (100 cm): resistant, light grey weathering, beige when fresh, massive, rubbly weathering, coarsely crystalline, dolomitized lime mudstone with bitumen and calcite filling intercrystalline porosity (bitumen emplaced first).

- unit 2 (up to 60 cm): resistant, brown-grey weathering, tan when fresh, up to 2 cm tabular-bedded, mm-scale laminated, medium to coarsely crystalline dolomitized lime mudstone (Figures 5 and 6). Laminae are cryptalgal to stromatolitic. The top of the unit is undulatory with up to 15 cm relief. Intercrystalline porosity is approximately 10%. Fractures are bitumen stained.

- unit 3 (127 cm): resistant, light grey weathering, medium grey when fresh, 0.5 to 2 cm tabular-bedded, mm-scale laminated, medium crystalline dolomitized lime mudstone (Figures 5 through 8). Bedding in the top 30 cm is slightly undulatory. The uppermost 4 beds are 2 to 3 cm thick. Intercrystalline porosity is approximately 10%.

- unit 4 (11 cm): resistant, light grey weathering, medium grey when fresh, alternating 1 to 5 mm beds of 1) discontinuously bedded, low angle cross-bedded to trough cross-bedded, coarsely crystalline peloid dolomitized grainstone and 2) finely crystalline dolomitized lime mudstone (Figures 5 through 8). Peloid layers contain bitumen in 25–30% interparticle porosity.

- unit 5 (10 cm): resistant, light grey weathering, brown-tan when fresh, low angle cross-bedded, medium crystalline, *Amphipora* dolomitized rudstone in a grainstone matrix (Figures 5 through 8). Porosity is interparticle and intercrystalline. Fractures are bitumen stained.

- unit 6 (90 cm): resistant, grey-black stained, light beige-grey weathering, buff coloured when fresh, massive interbedded 1) dolomitized stromatoporoid bindstone and 2) fine to medium crystalline, dolomitized stromatoporoid and brachiopod rudstone in a grainstone matrix (Figures 5 through 7, 9, 10). Tabular and lamellar stromatoporoids which form the dolomitized bindstone are up to 15 cm thick. Porosity is intercrystalline. Fractures are bitumen stained. Downstream, this unit outcrops in a series of small mounds, thickens to up to 100 cm and contains massive stromatoporoids.

Figure 5. Stratigraphic section for the measured locality of the Keg River Formation on the Firebag River. Labels FBR2-1 through -6 denote approximate thin section locations. Numbers 1 to 6 on the left of the lithology column denote the stratigraphic units described above.

Figure 6. View of measured section from the upstream end of the Keg River Formation outcrop on the Firebag River. Only a small sliver of unit 5 is visible from the photographer's point of view.

Figure 7. The top of unit 3, all of unit 4, and part of unit 5 from the Keg River Formation outcrop on the Firebag River. Laminae in unit 4 are low angle cross-beds and long amplitude trough cross-beds.

Figure 8. Close-up of unit 4 from the Keg River Formation outcrop on the Firebag River. Laminated texture is from low-angle cross-beds and trough cross-beds. The orange colouration is the reflection from a field notebook used to illuminate the face of the rock.

Figure 9. Close-up of the top of the exposed bioherm at the measured section in unit 6, Keg River Formation, Firebag River. Tabular stromatoporoids encrust and follow the topography of skeletal sand lenses.

Figure 10. Close-up of a tabular stromatoporoid from the biohermal facies of unit 6, Keg River Formation, Firebag River. Note the fine morphological detail preserved in this dolomitized fossil.

2.3 Thin-Section Analysis

Thin sections from six samples collected from the outcrop units were prepared and analyzed under plane-polarized light using a Zeiss Axio Imager.A2m microscope to supplement the observations made in the field. The stratigraphic position of the samples is shown in Figure 5. Thin sections were partially stained with alizarin red to distinguish calcite from dolomite. In addition to visual estimates of allochems, pores, and bitumen using comparisons to silhouette percent diagrams, thin sections were point-counted along three to five horizontal transects spaced at 1 mm intervals under 25x magnification. Descriptions and point-counting results for the analyzed thin sections in stratigraphic order from base to top are as follows:

FBR2-6 (from the middle of unit 1, Figure 11): vuggy, dolomitized lime mudstone with rare recrystallized fossil fragments and peloids. Fossil fragments are either brachiopods or bivalves. All allochems are barely visible because they are ghosted into the crystalline dolomite fabric. Burrows are also ghosted into the fabric and are 0.5 to 1 mm in diameter, horizontal, and unlined. The dolomitized matrix is anhedral to subhedral and is patchy in crystal size, usually very fine or fine to coarse. Subhedral isopachous dolomite surrounds some pores, usually only the large vugs. Botryoidal dolomite is patchy and rare, limited to one small area of the thin section. Botryoids are <0.5 mm in diameter. Pores are dissolutional and vuggy. Large pores, up to 5 mm, are usually lined with isopachous dolomite and bitumen. Most smaller pores, usually <0.5 mm in diameter, are not lined with isopachous rims. All small pores and 25% of large pores are open. 75% of the large pores are filled with blocky calcite. Differences in pore lining and cementation suggest two discrete pore-forming events. Many pores are lined with bitumen.

Point counts:

dolomite matrix: 103

open pore space: 22

blocky calcite (fills large vugs): 8

botryoidal dolomite: 2

bitumen: 3

skeletal allochem (recrystallized and dolomitized): 2

peloid (ghosted): 1
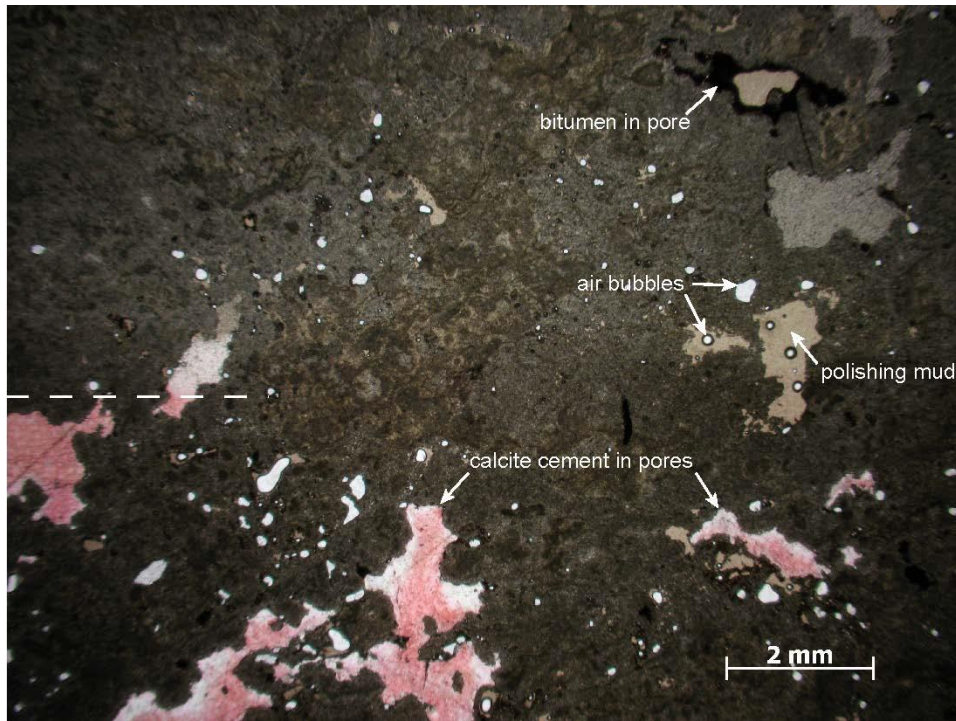
Figure 11. Thin-section photomicrograph of sample FBR2-6 from the middle of unit 1 photographed under plane-polarized light. Note the "clotted texture" of the mottled dark brown and light brown dolomitized micrite. Dark brown areas contain ghosted peloids, which contribute to the clotted texture. The lower half of the slide (below the dashed white line) is stained with alizarin red. Some porosity is filled with polishing mud (brownish-grey gritty texture, labelled) during the thin section preparation process. Bright white specks are air bubbles and holes created during polishing.

FBR2-1 (from the top of unit 2, Figure 12): dolomitized peloidal packstone to grainstone; peloids are ghosted into anhedral, very fine to medium crystalline dolomite fabric. Peloids are <0.3 mm in diameter and are visually 95% of the rock (excluding pore space). Some peloids are slightly compressed. Argillaceous stringers, up to a few mm in length, are dispersed throughout the sample and were displaced during recrystallization. Porosity is intercrystalline and dissolutional, possibly following original fenestral pore networks. Pores are up to 1 mm in diameter, randomly shaped, sub-horizontally oriented, and 95% of them are open. Porosity is highly variable and patchy, and visually estimated values range from 10 to 50%. Most pores are lined with bitumen and a few tiny pores are occluded by bitumen. Bitumen occupies about 1–2% of the rock volume.

Point counts:

dolomite crystalline matrix: 102

argillaceous wisps: 11

well-defined (not ghosted) peloids: 5

open pore space: 29

bitumen-filled pore space: 7
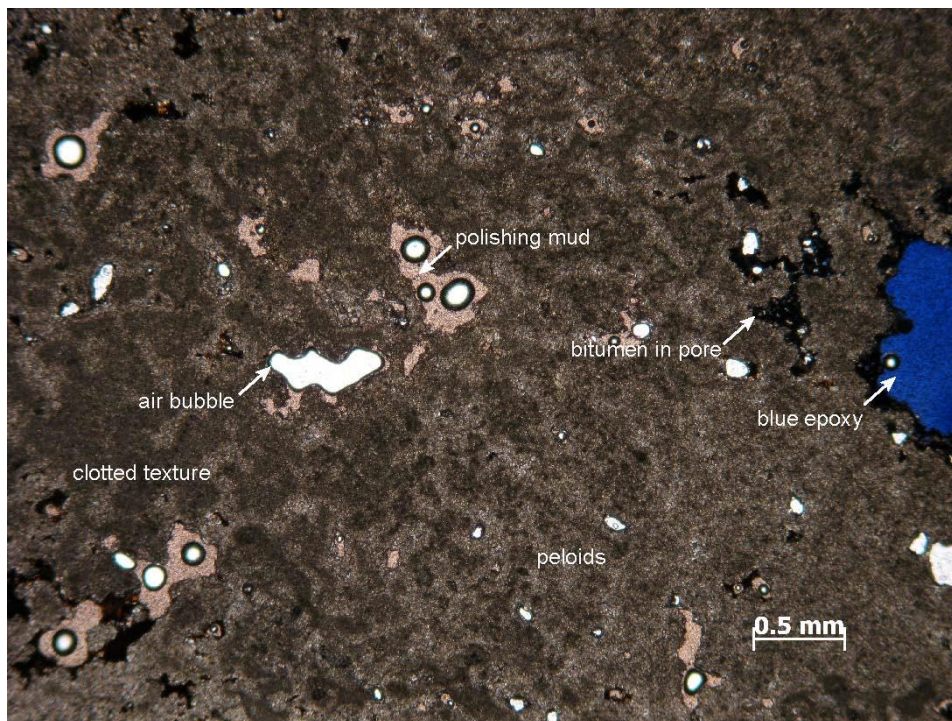
Figure 12. Thin-section photomicrograph of sample FBR2-1 from the top of unit 2 photographed under plane-polarized light. Peloids occur as abundant small, dark masses that amalgamated into a clotted texture. Bright white specks are air bubbles and holes created during polishing.

FBR2-2 (from 20 cm below the top of unit 3, Figure 13): laminated, dolomitized peloidal grainstone. Laminae alternate between densely packed, compressed peloids and less dense packing of uncompressed peloids. Peloids are <0.3 mm in diameter and are visually 90% of the rock (excluding pore space). In most peloids, only the cores are well-defined; the outer edges are obscured by dolomitization. Dolomitization of peloids is anhedral and very finely crystalline. Inter-peloidal dolomite is also anhedral but is very fine to finely crystalline. The coarsest crystals (usually fine, occasionally medium) line pores. Porosity is interparticle and intercrystalline, likely after original fenestral fabric. One 5 by 20 mm vug is present. Most pores are arranged along horizontal laminae or are defined by inter-peloidal space and are visually 10–20% of the rock, variable among laminae. Almost all pores are <1 mm; most are <0.5 mm diameter. Almost all pores are open, and many are lined with bitumen. Bitumen also occurs between peloids and along laminae and is visually <1% of the rock. One hairline fracture, 30 degrees from vertical, is open, likely originating from sectioning.

Point counts:

peloids (cores only): 106

crystalline dolomite (not in peloid cores): 36

open pore space: 5
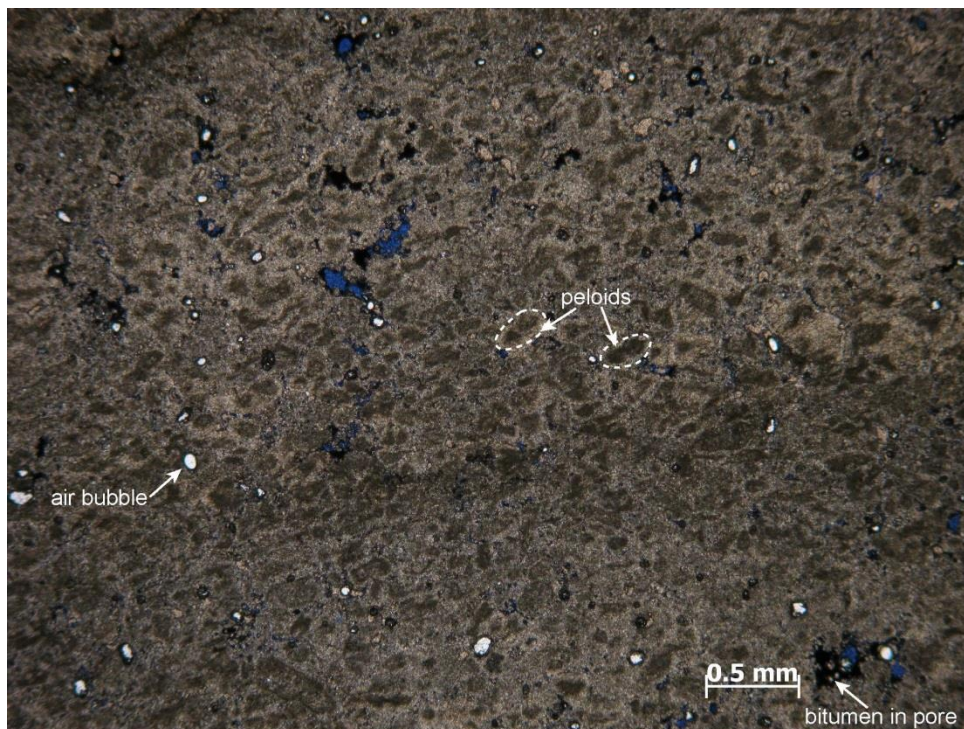
Figure 13. Thin-section photomicrograph of sample FBR2-2 from unit 3 photographed under plane-polarized light. Note the abundant peloids (dark brown spots; examples of two peloids are outlined with white dashes) and decreased porosity relative to other samples. Bright white specks are air bubbles and holes created during polishing.

FBR2-3 (from the middle of unit 4, Figure 14): laminated, dolomitized peloidal grainstone. Peloids are <0.3 in diameter and are visually 75–80% of the rock (excluding pore space). Dolomite is either euhedral to subhedral, fine to medium crystalline isopachous cement around peloids, or anhedral and very finely crystalline where it replaces the peloid cores. Peloids are cemented together by isopachous rims, possibly replacing both the peloid edges and original marine isopachous cement. Pore space is interparticle and dissolutional (mouldic, intra-peloidal). Pore shape and distribution is controlled by peloid distribution and shape. Porosity is visually 10–30% of the rock, variable among laminae. Most pores are <0.5 mm in diameter. All pores are open, but bitumen stains the rims of many pores. Bitumen occupies between 0 and 2% of the rock.

Point counts:

peloid cores: 89

open pore space: 47

isopachous dolomite cement: 18

bitumen: 2
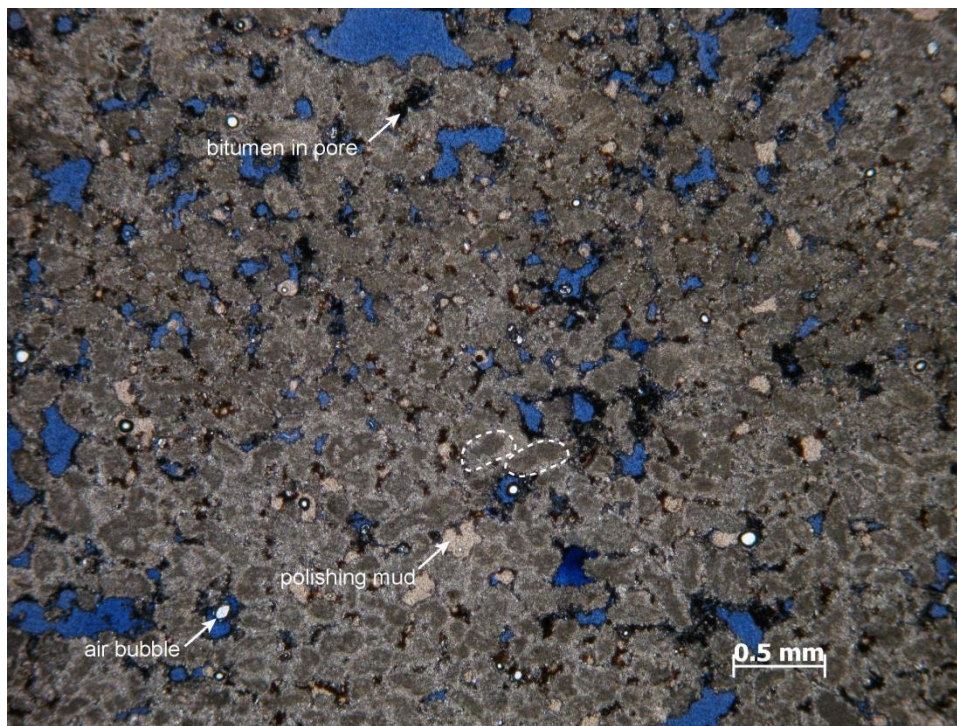
Figure 14. Thin-section photomicrograph of sample FBR2-3 from unit 4 photographed in plane-polarized light. Note the abundance of peloids and solution-enhanced, inter-peloidal pores. Two peloids are outlined in white, dashed lines as examples. Bright white specks are air bubbles.

FBR2-4 (from the top of unit 5): this sample contains two distinct lithologies: the lower half is a dolomitized, laminated, clotted mudstone (after altered peloidal packstone to grainstone); the upper half is a peloid-*Amphipora* packstone. This thin section crosses the boundary between the dolomitized laminated lime mudstone and dolomitized skeletal-peloidal grainstone. The boundary is abrupt, without evidence of scour, exposure, or any other disruption, and bitumen-stained.

Lower half (Figures 15 and 16): clotted peloid masses in which only the ghosted edges of peloids are preserved. Peloids deteriorated after burial to form a lime mudstone that was later dolomitized. One recrystallized brachiopod fragment was observed. Dolomite is present as pore-lining, fine to medium crystalline, isopachous cement, or is very finely to finely crystalline where it replaces peloids. Dolomite recrystallization displaced argillaceous material into discontinuous wisps of up to a few mm in length. Pore space is visibly 15–20% and occurs as interparticle porosity between peloids and as mouldic porosity in dissolved clusters of peloids. Pores are up to 2 mm in diameter, but most are <1 mm. All pore space is defined by allochem morphology and distribution. All pores are open. The edges of some pores are bitumen-stained.

Point counts:

crystalline dolomite (non-isopachous): 54

isopachous dolomite cement: 19

peloids (including clots of deteriorated peloids): 47

open pore space: 34

argillaceous wisps: 6

recrystallized brachiopod: 1
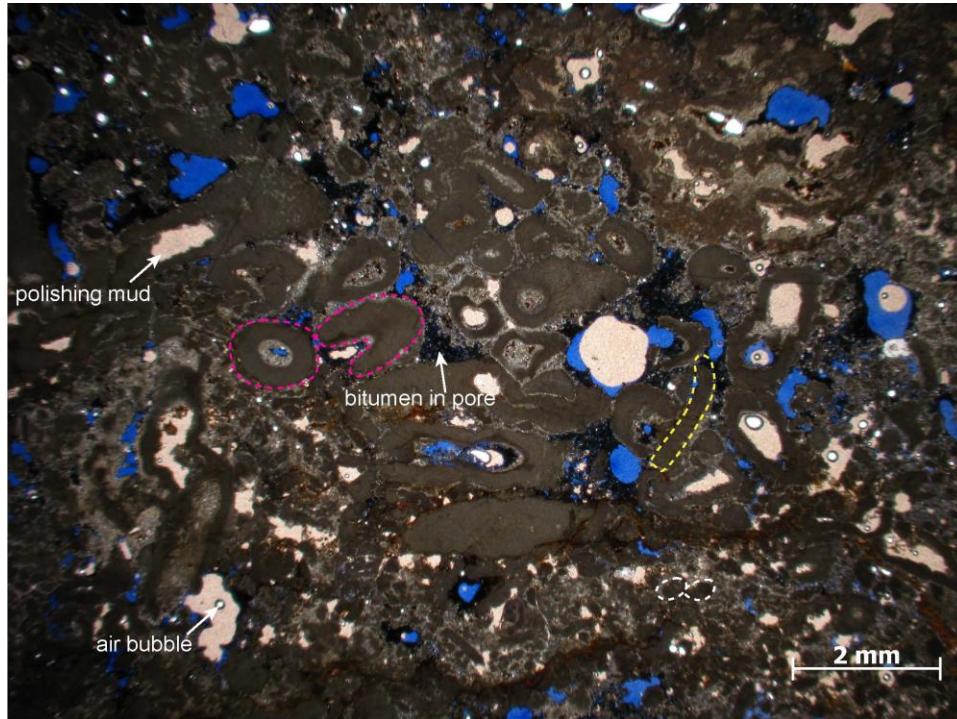
Figure 15. Thin-section photomicrograph of the lower half of sample FBR2-4 from unit 5 photographed under plane-polarized light. Dashed pink lines outline two examples of *Amphipora* segments; the yellow dashed line outlines an example of a brachiopod shell fragment, and the white dashed lines outline two peloids.
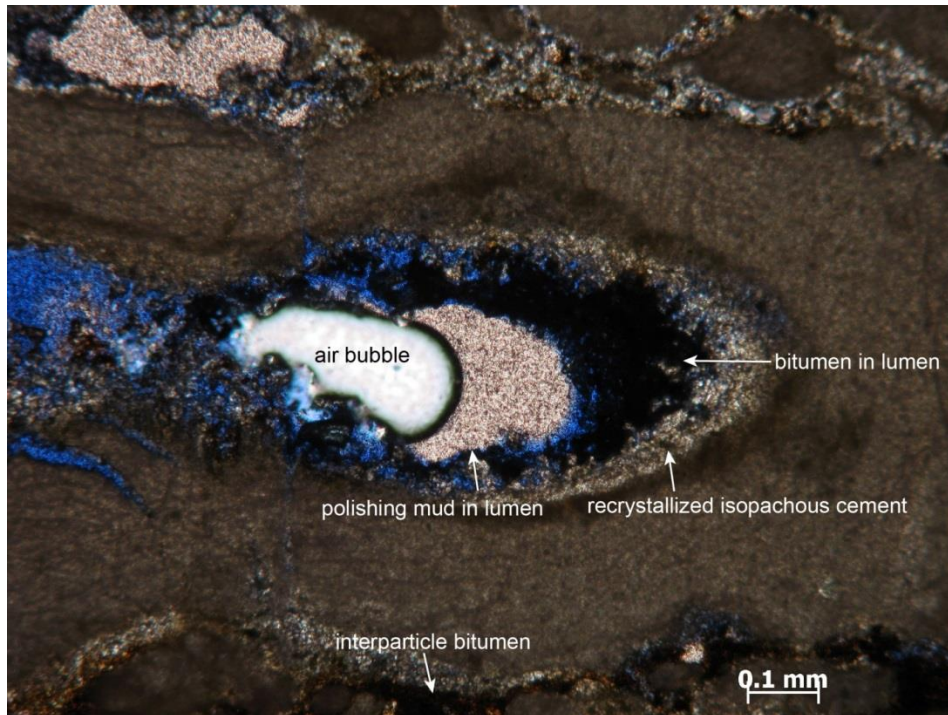
Figure 16. Close-up of an *Amphipora* segment in sample FBR2-4 photographed under plane-polarized light, showing recrystallized isopachous cement and bitumen in intra- and interparticle porosity.

Upper half (Figure 17): dolomitized and recrystallized *Amphipora* fragments and randomly oriented peloids cemented by isopachous cements which were altered to fine- to medium-crystalline, sub-hedral dolomite. Dolomitized botryoids were noted in an area <5 mm in diameter. Porosity ranges from 15–40% and is defined by allochem shape and distribution: interparticle between the isopachous rims around allochems, and intraparticle within *Amphipora* internal chambers. Pores are up to 2 mm in diameter, but most are <1 mm. All pores are open; some are stained with bitumen.

Point counts:

Amphipora: 41

peloids: 28

isopachous dolomite cement: 19

open pore space: 25

bitumen: 5
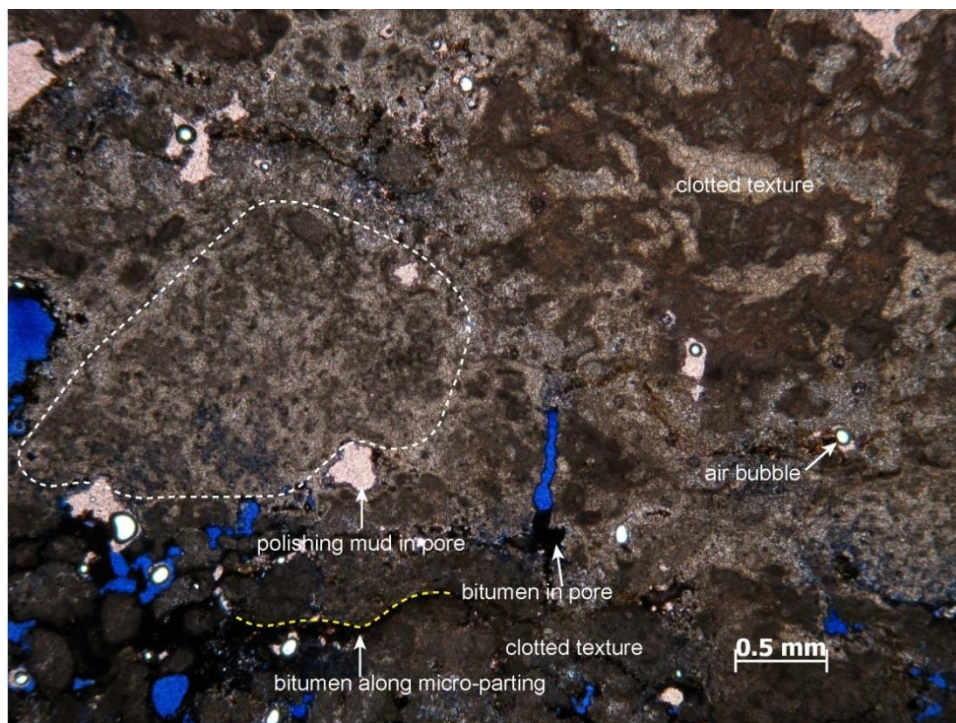
Figure 17. Thin-section photomicrograph of the upper half of sample FBR2-4 from unit 5 photographed under plane-polarized light. The white dashed line outlines an area of dense peloids. The yellow dashed line traces part of a micro-parting. Bright white specks are air bubbles.

FBR2-5 (from the top of unit 6): this sample has two lithologies: a) tabular stromatoporoid (seen in hand sample and outcrop) dolomitized to a laminated lime mudstone (seen in thin section), and b) dolomitized intraclastic grainstone to packstone. The two lithologies are interbedded at a cm-scale, including in-situ laminated mudstone and rip-up clasts of the laminated mudstone in the intraclastic grainstone to packstone.

Tabular stromatoporoid (Figures 18, 19, and 20): The dolomitized tabular stromatoporoid was dolomitized to anhedral to subhedral, fine to very finely crystalline dolomudstone and is either interbedded with the packstone to grainstone or forms the intraclasts (rip-up clasts) in the packstone to grainstone. Occasional, coarse to very coarse dolomite rhombs are present in the pore space between latilaminae (layers). Moulds of gypsum needles, radially to randomly oriented, form occasional patches along some latilaminae (Figure 20). Pore space is visibly up to 10% of the stromatoporoid and occurs between latilaminae, or is fracture or mouldic (after gypsum needles). Pores are up to 3 mm in length, the longest occurring along fractures. Some of the gypsum-needle moulds are filled with bitumen. Fractures are 1 to 3 mm in length and are subvertical to vertical within latilaminae, usually occurring as several within a single latilamina and opening upwards or downwards. Fractures do not appear to be caused by or related to original astrorhizal canals (stromatoporoid structures related to water flow). Fractures remain unfilled and uncemented.

Point counts:

stromatoporoid: 57

pore space (along latilaminae): 14

bitumen: occurring in the point-count field but not falling on points; along latilaminae
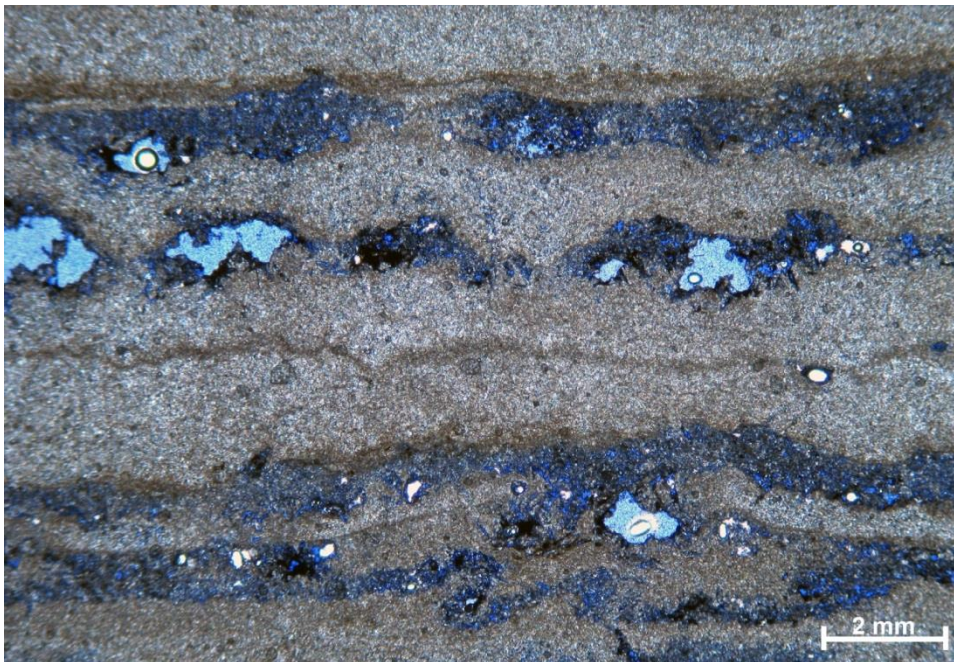
Figure 18. Thin-section micrograph of latilaminae of a dolomitized tabular stromatoporoid (beige layers) in sample FBR2-5 from unit 6 photographed under plane-polarized light. Pore space is blue. Bright white specks are air bubbles and holes created during polishing.
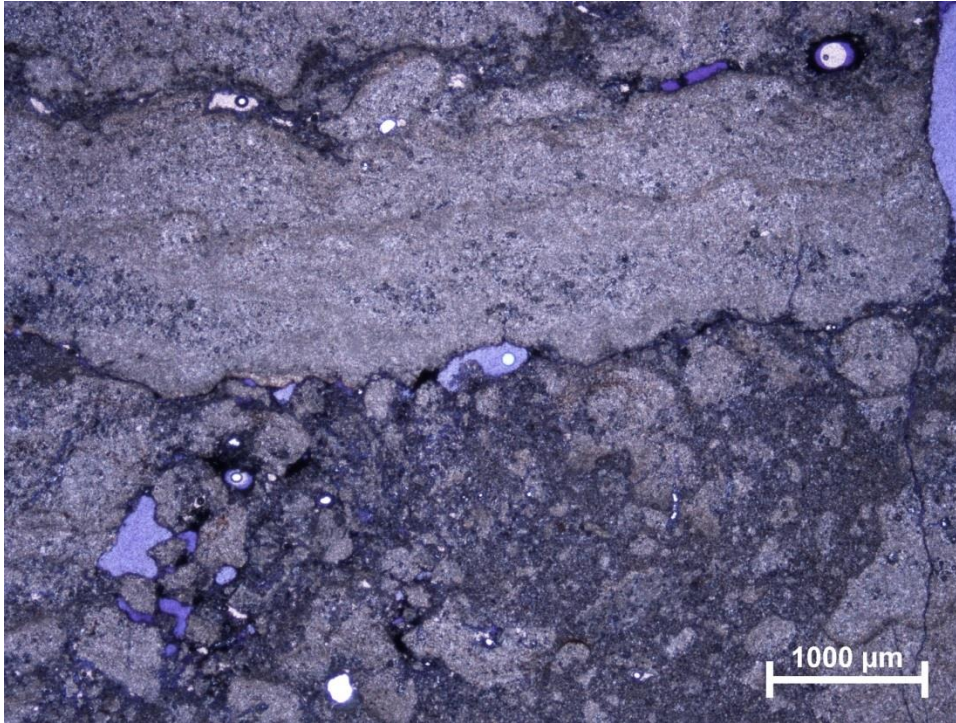
Figure 19. Intraclastic grainstone below tabular stromatoporoid latilaminae in thin section FBR2-5. White spots are pores formed during thin sectioning. Black is bitumen staining.
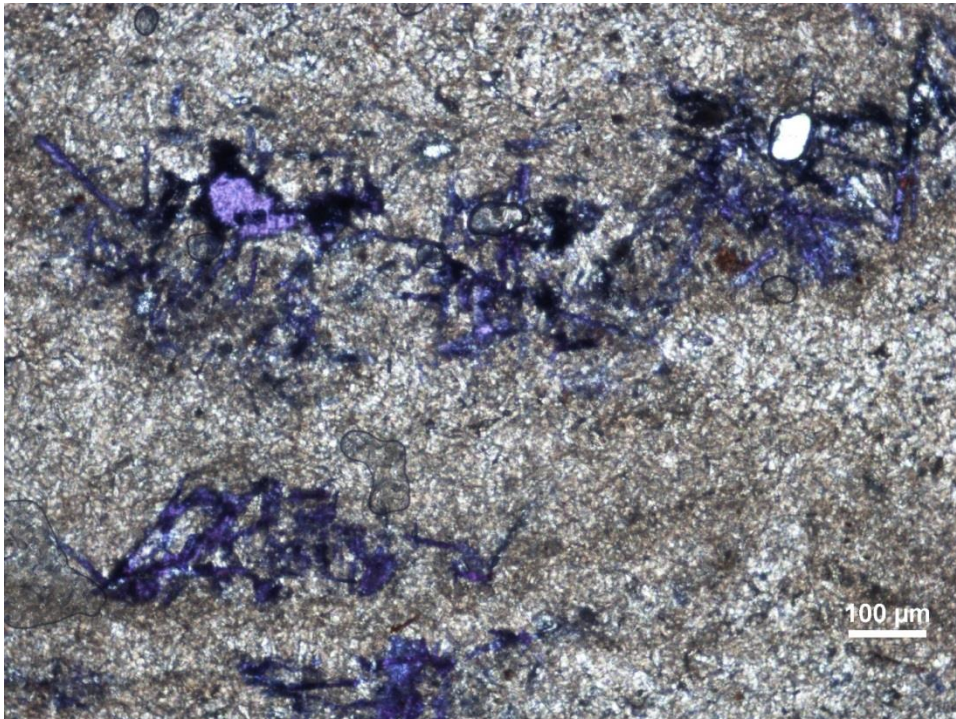
Figure 20. Gypsum needle mouldic pores in a latilamina of the tabular stromatoporoid, thin section FBR2-5. Most needles occurred in clusters, forming larger, irregular pores after dissolution, but some moulds retained their original needle-like shapes.

Intraclastic packstone to grainstone (Figures 19 and 21): the dolomitized packstone to grainstone was less resistant than the dolomitized stromatoporoid and so was more eroded during sectioning. Intraclasts from stromatoporoid latilaminae range from 30 mm in length to <1 mm in diameter (smaller intraclasts are randomly oriented) and are either floating in the recrystallized matrix or are touching. The anhedral dolomite of the packstone to grainstone matrix is very fine to finely crystalline, but was highly eroded during polishing of the thin section. Pore space, where determined to not arise from polishing of the thin section, was vuggy (vugs usually <0.5 mm) and up to 10% of the rock. All pores are open, but any fill of pore space may have been lost during the thin sectioning process.

Point counts:

matrix (deteriorated packstone to grainstone, allochems not defined): 53

intraclasts (lime mudstone rip-ups): 31

pore space (including pores in intraclasts): 15

unidentifiable allochems: 23

Amphipora: 2

bitumen (lining pore space): 1

angular quartz silt: occurring in the point count field but not falling on points; very rare
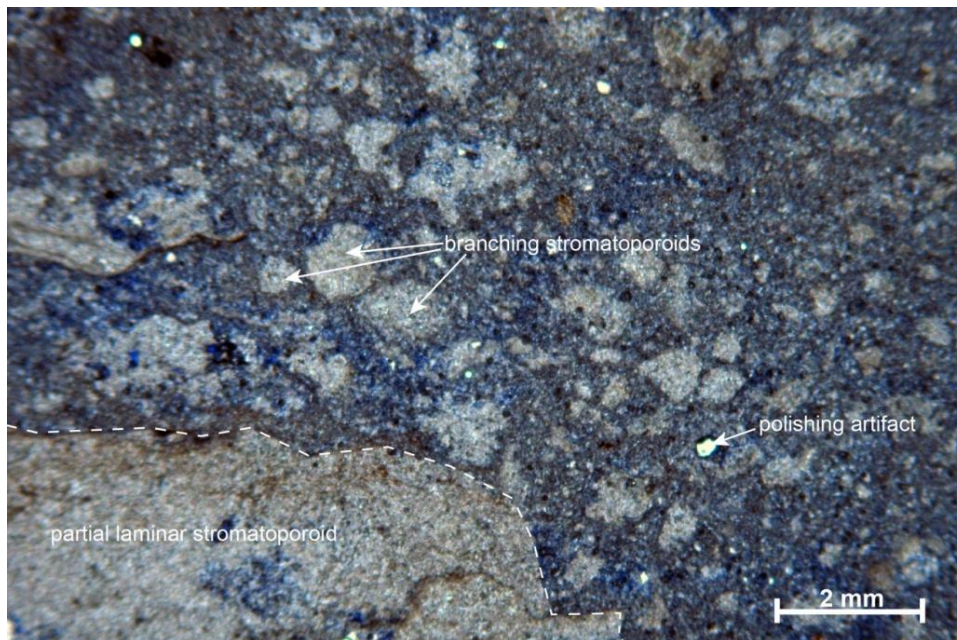
Figure 21. Thin-section micrograph of an *Amphipora* and other branching stromatoporoid pack- to grainstone in sample FBR2-5 from unit 6 photographed under plane-polarized light. Blue areas are pore space. Bright white specks are holes created during polishing.

2.4 Paleoenvironmental Interpretation

Lime mudstones described in the lower, laminated interval of the outcrop (units 1 through 4) were revealed to be peloidal grainstones in thin section. Dolomitization obliterated the outer edges of peloids but retained their cores; thus when the rock was observed in outcrop, only the crystalline matrix was seen. In thin section, the ghosted cores of peloids were apparent under the overprint of crystalline dolomite.

These laminated peloidal grainstones are interpreted to originate in the lower intertidal zone, perhaps in a quiet, shallow lagoon-like paleoenvironment. Abundant peloids attest to continuous biotic activity, possibly including bioturbation in some beds. The presence of gently undulose beds in outcrop, perhaps related to cryptalgal accumulation, further supports an intertidal origin for this interval.

The paleoenvironment abruptly shifts to a higher energy environment as you go upwards in the outcrop, observed in outcrop and in thin section FBR2-4 (unit 5). A skeletal-peloidal grainstone overlies the uppermost laminated, peloidal grainstone. This surface displays a sharp change in sedimentation without evidence of scouring, subaerial exposure, or hardground formation. The appearance of *Amphipora* in the grainstone attests to a shift in habitat from a quiet intertidal accumulation of peloids to one that is higher energy, perhaps a carbonate sand accumulation from wave activity, or a tempestite of *Amphipora* and other skeletal debris.

Above this, the marine paleoenvironment deepened and a small bioherm formed (unit 6). This bioherm was the expansion of the mounds seen in outcrops downstream along the Firebag River, prograding over the lagoonal sediments and the grainstone at this location as the lagoon deepened.

This outcrop exposes an internal lagoon within a biohermal complex, in which the slow deepening of the lagoon caused a shift from initially intertidal sedimentation to final biohermal growth. Internal lagoons within biohermal complexes are known from the Keg River Formation in subsurface within the region, sometimes even containing small evaporite deposits (D. Cotterill, pers. comm., 2016). In this outcrop, evidence of evaporites is minimal (rare gypsum needles growing in post-burial tabular stromatoporoids in sample FBR2-5).

In summary, excepting the lowermost unit, the outcrop contains one major transgressive sequence with two smaller-scale shallowing-upwards sequences in the shallow lagoonal to intertidal units of 2 and 3. Transgression after the termination of carbonate accumulation of unit 3 resulted in deposition of units 4 and 5 within the littoral to shallow sublittoral zone, likely within or just below fair-weather wave base. In the bioherm of unit 6, the presence of carbonate sand and the tabular to massive nature of the stromatoporoids suggests that the reef established above fair-weather wave base. Massive stromatoporoids formed the core of the bioherm while tabular stromatoporoids bound interstitial carbonate sands along the flanks of the bioherm.

2.5 Post-Depositional Alteration

After deposition, the carbonate sediments underwent cementation and lithification under marine conditions, as indicated by relict isopachous cements lining primary inter- and intraparticle pores and rimming allochems. Dolomitization and recrystallization resulted in the destruction of the original internal microstructures of fossils, but did not completely obliterate many primary sedimentary textures. Peloids were typically altered by dolomitization in the obliteration of their outer edges by recrystallization, but the cores of peloids, although dolomitized, remained sufficiently intact for identification. Bioturbation is suspected to be higher than reported (the only burrows observed under the microscope are in thin section FBR2-6), based on distribution of peloids, but primary burrow fabrics appear to be destroyed by dolomitization. In some samples, dolomite recrystallization resulted in the redistribution of small amounts of argillaceous or insoluble material, seen macroscopically as wisps up to a few millimetres in length. When viewed at high magnification (100x), this material appears to have been displaced by dolomite

crystal growth.

Pore types are variable, reflecting both pre- and post-cementation fabrics. Based on thin-section descriptions, the history of porosity includes

1) original fenestral and inter-particle porosity, occurring in peloidal and skeletal packstones to grainstones;

2) post-cementation dissolution of gypsum needles in thin section FBR2-5;

3) isopachous cementation of the walls of pores, insufficient to occlude pore space;

4) dissolutional enhancement of some pores which may obliterate isopachous cement and create mouldic porosity from some peloids, but timing with regard to dolomitization is unknown;

5) intercrystalline porosity, which formed during the alteration of limestone to dolostone and the coarsening of the matrix during the recrystallization process;

6) late-stage dissolutional porosity, seen in thin section FBR2-6, in which pinpoint pores (<0.5 mm) formed in the dolostone matrix;

7) calcite occlusion of larger vugs in thin section FBR2-6; and

8) petroleum migration through the rock, ultimately resulting in bitumen staining and fill of pores.

Fractures occur in only two thin sections. One set, in sample FBR2-5, occurs only in stromatoporoid latilaminae as vertical cracks. Many latilaminae are partially penetrated by a set of several of these cracks, all of which in a single lamina open upwards or downwards, but never in both an upward and downward orientation. These fractures are considered to be similar to syneresis cracks, formed during the shrinkage of the latilaminae after burial, and do not appear to be related to astrorhizal canals in the stromatoporoid.

A hairline fracture in thin section FBR2-2 is open and likely originated from sectioning, given that there are no cements or bitumen lining the walls of the fractures.

Bitumen occurs in all thin sections, primarily in pores, but sometimes along allochems or fractures. The amount of bitumen is variable between thin sections, ranging up to visibly 2% of the rock. The relationships between the bitumen, pore space, and calcite cement (thin section FBR2-6) suggests only one event of petroleum migration in the history of this outcrop.

3 References

Green, R., Mellon, G.B. and Carrigy, M.A. (1970): Bedrock geology of northern Alberta, NTS 84 and NTS74D, 74E, 74L, and 74M; east and west halves; Research Council of Alberta, AGS Map 024, two maps, URL <http://ags.aer.ca/publications/MAP_024.html> [August 2017].

Norris, A.W. (1963): Devonian stratigraphy of northeastern Alberta and northwestern Saskatchewan; Geological Survey of Canada, Memoir 313, 168 p., URL <http://geoscan.nrcan.gc.ca/starweb/geoscan/servlet.starweb?path=geoscan/fulle.web&search1=R=100540> [August 2017].

Schneider, C.L. and Grobe, M. (2013): Regional cross-sections of Devonian stratigraphy in northeastern Alberta (NTS 74D, E); Alberta Energy Regulator, AER/AGS Open File Report 2013-05, 25 p., URL <http://ags.aer.ca/publications/OFR_2013_05.html> [August 2017].

Schneider, C.L., Grobe, M. and Hein, F.J. (2013): Outcrops of the La Loche, Contact Rapids, and Keg River Formations (Devonian) on the Clearwater River: Alberta (NTS 74D/9) and Saskatchewan (NTS 74C/12); Alberta Energy Regulator, AER/AGS Open File Report 2012-20, 36 p., URL <http://ags.aer.ca/publications/OFR_2012_20.html> [August 2017].

Schneider, C.L., Grobe, M., Leighton, L.R., Hein, F. and Forcino, F.L. (2014a): Outcrops of the lower Waterways Formation (Firebag and Calumet members) on the Clearwater, Athabasca, and Firebag rivers, Alberta (NTS 74D, E); Alberta Energy Regulator, AER/AGS Open File Report 2014-08, 34 p., URL <http://ags.aer.ca/publications/OFR_2014_08.html> [August 2017].

Schneider, C.L., Mei, S., Haug, K. and Grobe, M. (2014b): The sub-Cretaceous unconformity and the Devonian subcrop in the Athabasca Oil Sands Area, townships 87–99, ranges 1–13, west of the Fourth Meridian; Alberta Energy Regulator, AER/AGS Open File Report 2014-07, 32 p., URL <http://ags.aer.ca/publications/OFR_2014_07.html> [August 2017].